Accepted Manuscript

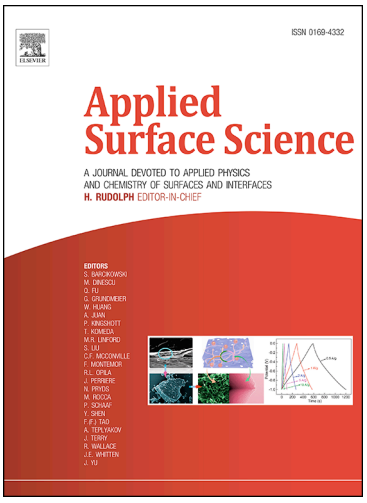

Full Length Article

Immediate release of helicid from nanoparticles produced by modified coaxial electrospraying

Deng-Guang Yu, Xiao-Lu Zheng, Yaoyao Yang, Xiao-Yan Li, Gareth R. Williams, Min Zhao

PII: S0169-4332(18)33486-X
DOI: https://doi.org/10.1016/j.apsusc.2018.12.147
Reference: APSUSC 41244

To appear in: *Applied Surface Science*

Received Date: 22 August 2018
Revised Date: 28 November 2018
Accepted Date: 14 December 2018

Please cite this article as: D-G. Yu, X-L. Zheng, Y. Yang, X-Y. Li, G.R. Williams, M. Zhao, Immediate release of helicid from nanoparticles produced by modified coaxial electrospraying, *Applied Surface Science* (2018), doi: https://doi.org/10.1016/j.apsusc.2018.12.147

Immediate release of helicid from nanoparticles produced by modified coaxial electrospraying

Deng-Guang Yu [a,*], Xiao-Lu Zheng [a], Yaoyao Yang [a], Xiao-Yan Li [a], Gareth R Williams [b], Min Zhao [c,**]

[a] *School of Materials Science & Engineering, University of Shanghai for Science & Technology, Shanghai 200093, China.*
[b] *UCL School of Pharmacy, University College London, 29-39 Brunswick Square, London WC1N 1AX, UK.*
[c] *School of Pharmacy, Queen's University Belfast, Belfast BT9 5AH, UK.*

Corresponding authors:
Address:
***DG Yu:**
School of Materials Science & Engineering,
University of Shanghai for Science and Technology,
516 Jungong Road, Yangpu District,
Shanghai 200093, P.R. China
Tel: +86-21-55270632
Fax: +86-21-55270632
Email: *ydg017@usst.edu.cn*

**** M Zhao:**
School of Pharmacy
Queen's University Belfast
Belfast BT9 5AH, UK
Email: *m.zhao@qub.ac.uk*

Abstract

In this paper, a modified coaxial electrospraying process was explored for the generation of novel nanoscale composite materials. A solution comprising 5% (w/v) of the model drug helicid and 10% (w/v) polyvinylpyrrolidone (PVP) K10 in a mixture of N,N-dimethylacetamide and ethanol (4:6, v:v) was employed as the shell working liquid. This could not be processed into a solid product when processed by single-fluid electrospraying. However, when undertaking co-axial electrospraying with a core shellac solution (40% w/v in ethanol) solid particles were obtained. An extremely thin nanocoating layer of drug-polymer composite with an estimated thickness of 7 nm was deposited on a shellac core. X-ray diffraction and infrared spectroscopy demonstrated that the drug was converted into an amorphous nanocomposite with the PVP in the shell layer, losing its original crystalline state. *In vitro* dissolution tests revealed that all the helicid loading could be released within one minute, suggesting the particles have potential applications to deliver very rapid therapeutic effects. Mechanisms are proposed underlying the formation and functional performance of the materials.

Keywords: Functional nanocoating; Modified coaxial electrospraying; Immediate release; Core-shell structures; Poorly water-soluble drug

1. Introduction

In the 21st century, materials at the nanoscale are widely explored in the research and development of functional materials in numerous applied fields [1,2]. Electrohydrodynamic atomization (EHDA, including electrospraying, electrospinning and e-jet printing), is a useful approach to making nanoscale objects using electrical energy [3-7]. The extensive and facile interactions which arise between liquids and electrical fields means that EHDA can not only generate materials at the micro-/nano scale but also create a series of complex nanostructures [8,9]. No matter how complicated the desired architectures are, they can be achieved simply in a single step based on the nozzle structure of the spray head (or spinneret) [10-12]. This capability of producing nanostructures from a macroscale template has allowed the advancement of complex nanostructures (particularly core-shell structures) in a wide variety of applied fields, and these applications have in turn promoted the development of increasingly sophisticated EHDA processes such as side-by-side [13], tri-axial [14,15], modified tri-axial [16-18], and quartet-axial [19].

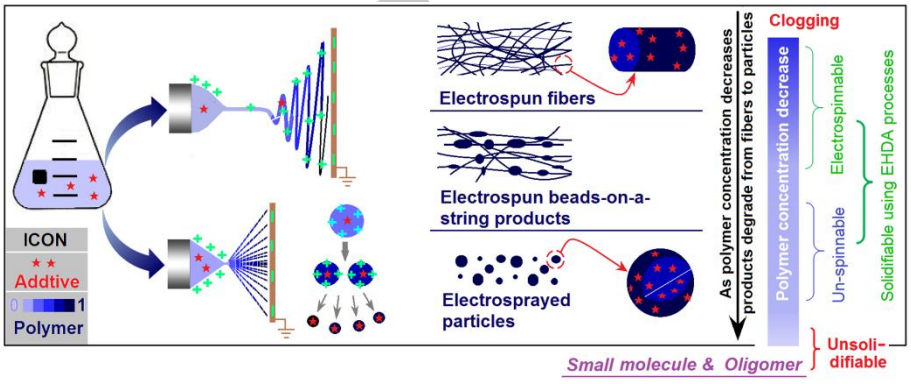

Fig. 1 The fluids that can be treated using EHDA processes. These include polymer-based liquids, and also solutions containing small molecules or oligomers.

A polymer with good filament-forming properties can be processed into nanofibers (through electrospinning), beads-on-a-string fibers, or solid particles (through electrospraying) (Fig. 1), moving from the former to the latter as the concentration of polymer in the working fluids decreases. Hence, the EHDA working fluids can be divided into different classes: those which cannot be processed due to clogging of the spinneret

(resulting from an extremely higher concentration), electrospinnable (often within a suitable concentration range), unspinnable but solidifiable (solid particles), and unsolidifiable (no solid product) when extremely dilute solutions are used [20,21]. In the simplest monoaxial EHDA process, the active ingredients can be encapsulated directly into polymers and also inorganic materials in one step [22,23]. In multiple-liquid EHDA processes, which are employed to create complex nanostructures, the possibilities are further expanded. On one hand, multi-liquid EHDA has led to the successful preparation of numerous complex nanostructures such as core-shell, Janus, and tri-layer systems, as well as products which combine core-shell and Janus features [12-19]. On the other hand, many new working fluids can be processed in the multi-liquid approach. These includes those which are un-spinnable (i.e. cannot be electrospun into nanofibers alone), un-solidifiable (cannot be electrosprayed into particles alone) [24-27]. These un-spinnable/un-solidifiable fluids often consist of polymers without filament-forming properties, oligomers, or small molecules. Their inclusion in the EHDA processes has permitted the appearance of a series of new multiple-fluid EHDA processes (such as modified coaxial and modified tri-axial electrospinning/electrospraying), and novel nanostructures.

Since the first report into coaxial EHDA [28], it has been recognized that if the shell working fluid can be converted into nanofibers or particles when treated using a monoaxial process (i.e. a solidifiable solution in Fig. 1), solid products can be generated from a coaxial method regardless of whether the core fluid is solidifiable or un-solidifiable. For example, a recent publication reported core-shell particles with oil encapsulated by a solid shell [29]. In this case, the core fluid alone cannot be processed into solid particles by EHDA, but when paired with a shell solution which is solidifiable a solid product is obtained [29]. If only the un-solidifiable fluid was used for the experiment, the resultant product would be a wet film rather than solid particles. This is generally undesirable, although such films can sometimes be useful: for instance, Yang et

al. have applied EHDA to such an un-solidifiable polyacrylonitrile (PAN) fluid and exploited this to generate solid carbon foams [30]. There remains however a lack of understanding as to whether solid core-shell particles can be prepared using un-solidifiable solutions as the shell working fluid. If this were to be possible, it would pave a new way for developing many functional core-shell materials, because it would allow functional components to easily be coated on a solid core to take advantage of their large surface areas.

The core-shell structure, comprising two different sections with an inner-outer spatial relationship, is probably the most commonly used starting point for designing functional nanomaterials [31-33]. In pharmaceutics, it can provide a series of strategies for resolving challenges such as avoiding an initial burst release, protecting easily-degraded drugs from the environment, targeting release, and manipulating spatiotemporal drug release profiles [34-38]. To the best of our knowledge, there are no reports where electrosprayed particles have been prepared using a drug-loaded shell to control the drug release profile and where the core section serves as a support. Such a formulation could potentially be very beneficial, because a thin shell layer will have a very large surface area-to-volume ratio, allowing very rapid release of the drug. Given the large number of poorly-soluble class II and IV active ingredients, a number of applications can be envisaged in terms of enhancing bioavailability [39-41].

For many poorly soluble drugs, a rapid release is required for optimum therapeutic efficacy, for instance in the treatment of conditions such as heart attacks, depression, high fever, and extreme pain [42]. As a result, immediate and fast-dissolving drug delivery systems have been rapidly developed in the industrial sector (e.g. immediate release tablets or capsules and oral fast-dissolving films). Much scientific research has also been devoted to this topic, with the exploration of new methods to fabricate high-performance formulations (e.g. electrospinning, 3D printing, and combinations with traditional pharmaceutical strategies) [43-46].

In this work, a modified coaxial electrospraying process was developed to produce core-shell nanoparticles in which the shell comprised a thin layer of helicid and polyvinylpyrrolidone (PVP). This solution alone could not be solidified using EHDA, but core/shell materials could be generated through use of a core fluid containing the natural biopolymer shellac. Shellac has been widely utilized as a coating material on food products [47,48], and also in the pharmaceutical industry to give sustained and colon-targeting release [49]. It is easily processed by EHDA, and both electrospun nanofibers and electrosprayed particles can be fabricated [50,51].

Helicid, 4-formylphenyl-O-β-d-allopyranoside, is an active ingredient extracted from seeds of the Chinese herb *Helicia nilagirica*. It has been clinically utilized to treat diseases such as vascular headaches, neurasthenia, and trigeminal neuralgia [52-54]. At ambient temperature, helicid is insoluble in water and in many organic solvents such as ethanol, acetone, chloroform, and methanol [53]. It thus suffers from poor bioavailability in vivo. Helicid is also challenging to process by EHDA: although it is soluble in N,N-dimethylacetamide (DMAc), the high boiling point of this solvent (166 ^{o}C) makes it very difficult to process helicid solutions using EHDA. In this work, we were able to use the presence of the solidifiable core solution to both process a helicid solution and also generate a fast-dissolving drug-loaded nanocomposite for the rapid relief of symptoms.

2. Materials and methods

2.1. Materials

Shellac (98%, wax free) was provided by the Sheng-Hui Agricultural Sci & Tech Co., Ltd. (Yun-Nan, China). Polyvinylpyrrolidone (PVP) K10 (molecular weight 10,00 Da) was obtained from the Shanghai Sigma-Aldrich Co., Ltd. (Shanghai, China). Helicid was bought from Winherb Medical Science and Technology Co., Ltd. (Shanghai, China). The required solvents (analytical grade) including acetone, DMAc, and anhydrous

ethanol, were purchased from the Shiyi Chemical Reagent Co., Ltd. (Shanghai, China). Water was double-distilled before use.

2.2. Co-axial electrospraying

All the electrospraying processes were carried out using a self-made electrospraying system, which consisted of two pumps (KDS100, Cole-Parmer, Vernon Hills, IL, USA), a power supply (ZGF2000, Wuhan Hua-Tian Co., Ltd., Wuhan, China), a collector and a coaxial spray head. A diagram about the homemade spray head is shown in Fig. S1 in Supplementary Information. Experiments were performed at a temperature of 21 ± 4 °C and a humidity of 54 ± 7%.

The core fluid was prepared by dissolving 40 g shellac into 100 mL ethanol. The shell fluid was composed of 5 g helicid and 10 g PVP K10 in 100 mL of DMAc and ethanol (40:60, v/v). After some preliminary experiments, the applied voltage and the particle collection distance were fixed at 20 kV and 15 cm, respectively. Two sets of particles were prepared, one from monoaxial electrospraying of the core fluid at a flow rate of 1.0 mL/h (denoted P1), and one using the modified coaxial process (P2). For the latter, the shell and core fluid rates were 0.2 and 0.8 mL/h, respectively.

2.3. Morphology and internal structure

The morphology of P1 and P2 were assessed using a Quanta FEG450 scanning electron microscope (SEM, FEI Corporation, Hillsboro', OR, USA). The particles were spread on a conductive adhesive, and then were platinum sputter-coated for 60s under a N_2 atmosphere. The ImageJ software (NIH, Bethesda, USA) was used to estimate the average diameters of the particles through over 100 measurements in SEM images. The inner structure of P2 was investigated using a transmission electron microscope (TEM, JEM2100F, Tokyo, Japan). Particles were collected directly on a lacy carbon-coated copper grid during the modified coaxial electrospraying process.

2.4. Physical form and component compatibility

A D/Max-BR diffractometer (Rigaku, Tokyo, Japan) was utilized to obtain X-ray diffraction (XRD) patterns over the 2θ range 5 to 60°. The X-ray was supplied with Cu Kα radiation at 40 mV and 30 mA. A Spectrum 100 spectrometer (PerkinElmer, Billerica, MA, USA) was employed to collect Fourier transform infrared (FTIR) spectra, which were recorded between 500 to 4000 cm^{-1} at a resolution of 2 cm^{-1} .

2.5. Functional performance

2.5.1. *Drug loading and encapsulation efficiency*

0.2 g of the P2 particles was fully dissolved into 100 mL of phosphate buffered saline (pH=8.0, PBS, 0.1M) under heating at a temperature of 80 ^{o}C. After appropriate dilution, the helicid concentration was measured at λ_{max}=270 nm using a ultraviolet-visible spectrophotometer (UV-2100, Shanghai Unico Instrument Co., Ltd., Shanghai, China).

The drug loading (*DL*) and encapsulation efficiency (*EE*) were calculated according to the following equations:

$$DL=W_{hm}/W_{pm}\times 100\% \quad \text{(Equation 1)}$$

where W_{hm} and W_{pm} are the measured weight of helicid and the drug-loaded particles, respectively.

$$EE=W_{hm}/W_{hc}\times 100\% \quad \text{(Equation 2)}$$

where W_{hc} is the theoretically calculated weight of helicid in the particles.

2.5.2. In vitro dissolution tests

Following the Chinese Pharmacopoeia (2015 Ed.), in vitro dissolution tests were carried out using the paddle method on an apparatus with 6 vessels (RCZ-8A, Tian-Jin University Radio Factory, Tian-Jin, China). 900 mL of PBS (pH 7.0, 0.1M) was added to each vessel and heated at 37 ± 1 ^{o}C with a rotation rate of 50 rpm. After the temperature was allowed to stabilize for 10 minutes, equal to 0.1g helicid of particles P2 (i.e. 3.5g P2) or 0.1g raw helicid powders were added. At predetermined time points, 5 mL of the dissolution medium was withdrawn and filtrated through a 0.22 μm membrane (Merck Millipore, Burlington, MA, USA). 5 mL of fresh preheated PBS was added into each vessel to maintain a constant volume. All measurements were conducted in triplicate, and are reported as mean ± S.D.

3. Results and discussion

3.1. The modified coaxial electrospraying

A schematic diagram of the coaxial electrospraying process is shown in Fig. 2. As for all EHDA process, it comprises four key components. The most important element is

the spray head, which determines the architecture of the product to be generated (e.g. an uniaxial metal capillary for a monoaxial electrospraying, a concentric spray head for coaxial electrospraying, a side-by-side spray head to produce Janus particles, or a tri-layer spray head for tri-axial electrospraying). One, two or more syringe pumps are used to supply the working fluids to the spray head, from which the fluids are guided into the electrical field in an organized manner. The third component is a high voltage generator, required to produce an electrical field. Finally, a grounded collector is positioned opposite the spray head.

In modified coaxial electrospraying, the core fluid is solidifiable. Thus, when the un-solidifiable shell solution flow was set to zero, monolithic solid particles can be generated solely from monoaxial spraying of the inner working fluid. When the shell fluid is switched on (i.e. F_s>0), a modified coaxial electrospraying experiment is conducted. If there were no solutes in the shell fluid, monolithic particles comprising solute(s) from the core fluids would be produced. Although it is not carried through into the products, the shell solvent can nevertheless aid the EHDA process (e.g. helping to prevent any clogging at the spinneret), and has an influence on the resultant particles in terms of their size and shape [20, 21, 24]. When there are solutes in the shell fluids, the resulted particles will comprise solid core-shell systems, with e.g. a nanocoating of functional ingredients at the surface.

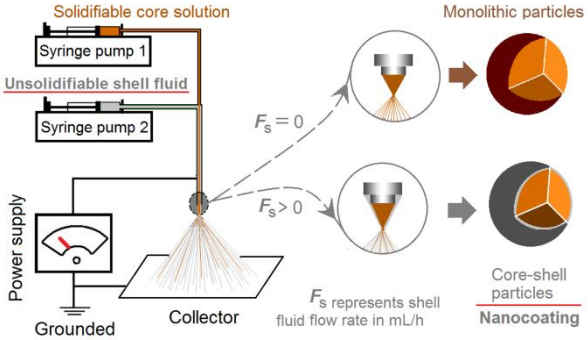

Fig. 2 The modified coaxial electrospraying system and the products that can be produced .

Fig. 3A shows the arrangements of the apparatus used in this work. A digital photograph of the home-made coaxial spray head is shown in Fig. 3B. This is composed of two capillaries. The smaller stainless steel capillary (having outer and inner diameters of 0.42 mm and 0.21 mm, respectively) projects out from the larger one (outer and inner diameters of 1.25 mm and 0.84 mm, respectively) to give a coaxial outlet. The projection length was 0.5 mm, which should be help to prevent mixing of the core and shell liquids. A crocodile clip was employed to connect the electrostatic energy from the power supply to the working fluids (Fig. 3C).

One-fluid electrospraying of the shell drug-PVP solution did not result in any solid particles, but only wet films. This is because of the low volatility of DMAc, whose boiling point was 166 ^{o}C. The Taylor cone observed during monoaxial electrospraying of the core fluid only is given in Fig. 3D. When the shell fluid was switched on, a typical coaxial process was recorded as depicted in Fig. 3E. The compound Taylor cone is exhibited in Fig. 3F: the brown-colored shellac core fluid and the transparent shell fluid can be clearly discerned.

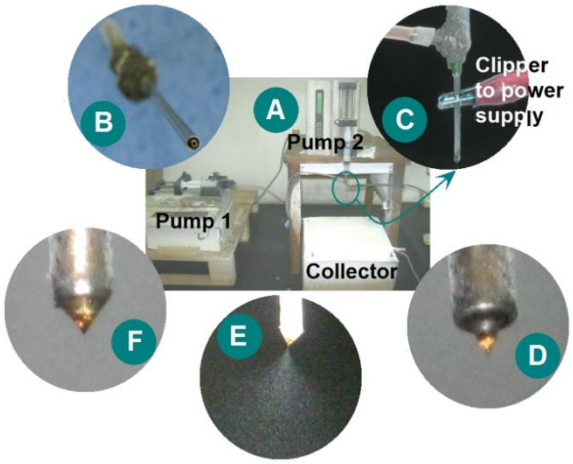

Fig. 3 The electrospraying apparatus and observations of the working processes: (A) the components of the coaxial electrospraying apparatus, (B) the concentric spraying head, (C) the connection of the high voltage to the spray head, (D) the single-fluid electrospraying process conduced with the core

shellac solution, (E) the double-fluid coaxial electrospraying process resulting from turning the shell solution flow on, and (F) the compound Taylor cone from (E).

3.2. Particle morphology and internal structure

For a given polymer, both electrospun fibers and electrosprayed particles can be achieved with an appropriate selection of solvent and working conditions (Fig. 1). Many polymers have both an electrospinnable concentration window in each solvent (where fibers can be generated), and should also have a solidifiable window within which solid particles can be fabricated. With ethanol as the solvent, at concentrations (w/v) between 70 to 90% shellac fibers are produced [55]. Concentrations between 20 to 35% w/v result in particles, and at intermediate concentrations between 35 to 70% the products often have a beads/spindles-on-a-sting morphology.

In this work, the core shellac had a concentration of 40% (w/v), which was intentionally selected to be slightly higher than the usual particle-forming concentration. An SEM image of the resultant P1 particles is shown in Fig. 4A. They have a morphology in which there are clear tails on the particles. The diameters of the latter are 1.21 ± 0.25 μm. When the modified coaxial process was carried out to yield P2, the particles generated had a spherical morphology with smooth surfaces (Fig. 4B). These particles had a diameter of 710 ± 80 nm (Fig. 4C), smaller than the pure shellac particles. A TEM image of P2 is exhibited in Fig. 4D. It is clear that a thin shell layer is coated on the core shellac. The thickness of this layer varied between 2 and 15 nm.

The polymer solutions often have a concentration range for solidification under a certain electrospraying condition. An intentional selection of a higher concentration of the core shellac fluid than its upper limitation (40%>35%, w/v) could remedy the un-solidifiable property of shell working fluid, ensuring a successful preparation of the core-shell nanostructures. Certainly, the shell-to-core fluid flow rate ratio became a very important parameter during the modified coaxial electrospraying processes. An enlarged shell-to-core ratio of 0.3/0.7 mL/h resulted in apparent aggregation of the electrosprayed

particles (Fig. S2 in Supplementary Information). Thus, on one hand, only one fluid must be solidifiable during the coaxial process. Loscertales and his co-workers demonstrated that the unsolidifiable oil could be encapsulated by a solidifiable polymer solution using a traditional coaxial process early in 2002 [28]. Here, a modified coaxial process shows that an un-solidifiable liquid could be explored as a shell fluid with a core solidifiable solution for creating a solid thin functional layer. On the other hand, the additional un-solidifiable shell solution should modify the electrospraying process in a favorable manner when a suitable fluid rate was selected. It is well known that electrons always aggregate on the surface of droplets [56]. As the applied voltage increases to create a larger surface electrostatic repelling force than the surface tension of the shell liquid, the electrospraying process should initiate the Columbic splitting for atomization of the working fluids. An un-solidifiable shell solution means smaller surface tension and more solvent at the air-liquid dynamic interfaces, which in turn means an easy splitting of the droplets and long time period atomization. Thus, the nanoparticles P2 not only had no tails of shellac particles P1, but also had an apparently smaller average diameter.

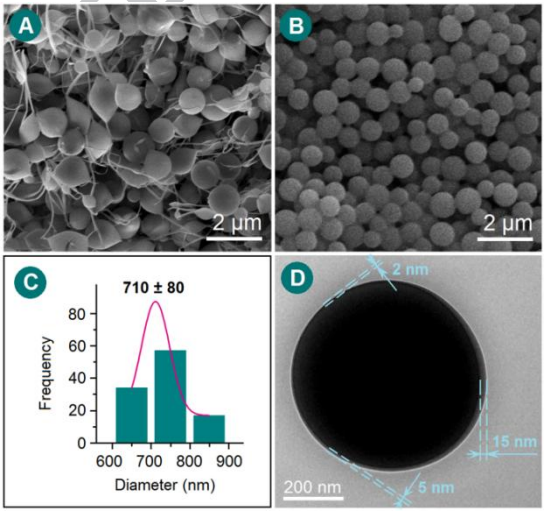

Fig. 4 Electron microscopy images of the electrosprayed particles: (A) SEM of the shellac P1 particles, (B) SEM of P2 particles generated by the modified coaxial processes, (C) the size distribution of P2, (D) a TEM image of P2 showing its core/shell structure.

3.3. Physical forms and component compatibility

XRD patterns and optical microscopy images of the raw materials and XRD data for the electrosprayed particles are presented in Fig. 5. As expected for a crystalline drug, the helicid pattern contains many sharp Bragg reflections, and a bright colorful image is seen under polarized light in optical microscopy. In sharp contrast, PVP K10 is transparent under the polarized light, while pure shellac can be seen to comprise brown flakes by the naked eye. These polymers are amorphous materials, as indicated by the presence of only broad haloes and a lack of Bragg reflections in their XRD patterns. The electrosprayed P2 nanoparticles (NPs) have an XRD pattern closely resembling those of the polymer raw materials. There are no sharp peaks visible, suggesting that helicid formed amorphous composites with the shell drug carrier PVP K10. These results were similarly verified by differential scanning calorimetry analyses (Fig. S3 in Supplementary Information).

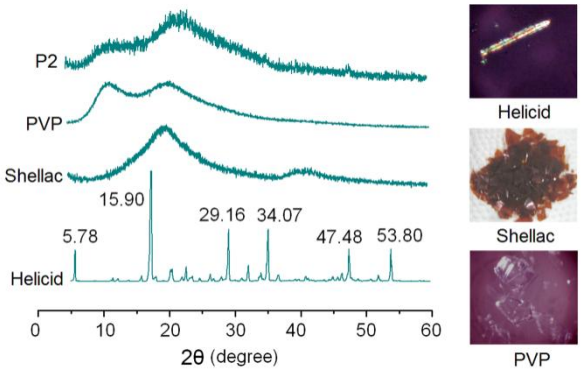

Fig. 5 XRD patterns of the raw materials and electrosprayed P2 nanoparticles (NPs), with optical images of the raw materials.

The compatibility between the components in the formulation will be important for their long-term stability. FTIR spectra of the raw materials and the P2 particles are depicted in Fig. 6A and 6B. The molecular structures of PVP, helicid and shellac are included in Fig. 6C.

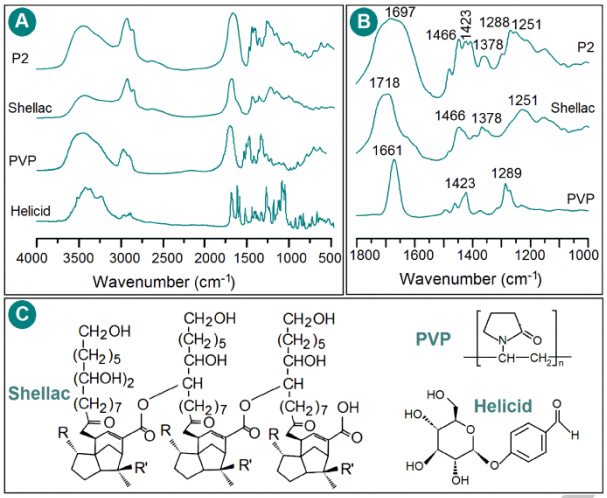

Fig. 6 FTIR spectra of the raw materials and P2 (A and B), and the molecular structures of PVP, helicid and shellac (C).

From Fig. 6A, it is clear that many sharp peaks in the spectra of raw helicid have disappeared in the spectra of particles. This indicates that PVP and helicid were converted into a molecular composite. This is sensible based on their chemical structures: there are five -OH groups in each helicid molecule and numerous -C=O groups within the PVP molecules. Thus, there are many opportunities for hydrogen bonds to form between helicid and PVP molecules, which is favorable for their compatibility.

Fig. 6B is an enlargement image of the 1800-1000 cm^{-1} region of Fig. 6A. The stretching vibration of -C=O lead to absorbance at 1661 and 1718 cm^{-1} for raw PVP and shellac, respectively. In contrast, the P2 particles exhibit a broad peak in this region with maximum absorbance at 1697 cm^{-1}. This is expected to be a composite of the C=O vibration from PVP and shellac. Other peaks present in the spectra of PVP (1423 and 1289 cm^{-1}) and shellac (1466, 1378 and 1251 cm^{-1}) are seen in the spectrum of P2, however. These observations suggest that the shellac (although its molecules have many -OH groups) and PVP present in the particles exist in a separate manner with minimum interactions between them: that is, the P2 system comprises a shellac core with a drug-PVP shell.

3.4. Functional performance

The measured contents of helicid in 0.2 g of the core-shell P2 particles was 5.648 ± 0.513 mg. Thus, the *DL* is about 2.824 ± 0.257 %. The drug loading is relatively low, suggesting that the particles will be potent only for poorly water-soluble drugs with low doses and high efficacy.

The theoretical mass of helicid in the particles can be calculated according to the concentrations of solutes in the working fluids and their flow rates: {(0.2 mL/h×5%)/[0.2×(5%+10%) + 0.8×40%]}×100%=2.857%. The *EE* is thereofre 5.648/5.714×100%=98.84%. This is as expected: EHDA methods comprise very fast drying processes, during which the solvents are evaporated and the solutes are converted into solid fibers or particles. Unless there is precipitation during the process, or significant absorption to the syringe used to dispense the spinning fluid, there should be minimal loss of drug during electrospraying. This is a significant advantage of EHDA over many bottom-up methods.

To demonstrate the release of drug from the P2 shell, a drop of water was deposited on the particles. After drying in air, the samples were Pt-coated and imaged by SEM (Fig. 7A and 7B). It is evident that the addition of a very small amount of water can dissolve the shell, and the helicid in the system then seems to re-crystallize into nanoparticles, as indicated by small dots at the surface of the particles in Fig. 7B.

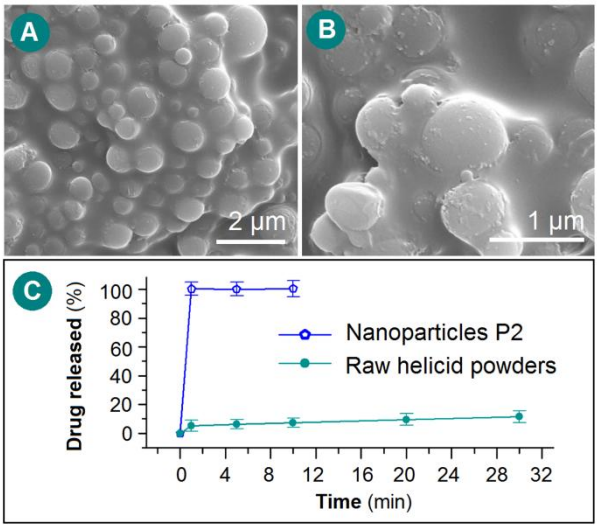

Fig. 7 The hydrophilicity of the P2 particles and the results of *in vitro* dissolution tests: (A) and (B) SEM images taken at different magnifications after a drop of water was applied to the particles, (C) the *in vitro* helicid release profiles from P2 and the raw drug powders (n=3).

The *in vitro* drug release profiles are given in Fig. 7C. The helicid in the P2 particles was released very rapidly, within one minute. In contrast, the raw helicid particles freed only 11.4 ± 4.2% of their drug content into the dissolution medium after 30 min, suggesting that the nanocoating led to a 263-fold (30×100/11.4) increase in the release rate over the raw drug powder.

3.5. Structure-performance relationship

In the single-fluid electrospraying process explored in this work, is clear that the droplets ejected from the syringe were deformed into a Taylor cone, which then breaks up into near-monodisperse droplets during the Coulombic explosion. The droplets quickly shrink as they travel toward the collector because of rapid solvent evaporation. The interactions of the electric field with the solvent accelerate the evaporation. This ensures the solvent is exhausted and completely solidified into the final products. When the un-solidifiable shell fluid is added to the system, atomization will mainly be controlled by the properties of this solution [18], and this will split evenly across the particles as the atomization and drying process proceeds. This will continue until there is an even coating on the dried shellac particles (Fig. 8).

In traditional coaxial electrospraying, the core fluid may or may not be solidifiable, but the shell fluid must be solidifiable. The latter dominates the drying process. In the modified coaxial processes, the shell fluid can be an un-solidifable liquid. This can be expected to keep the dispersed droplets in a fluid state for a relatively longer time period than when the shell is solidifiable. As a result, the droplets will continue to divide for a longer period of time, thus resulting in them dividing more times and ultimately yielding smaller particles. In this study, the un-solidifiable helicid-PVP shell solution leads to the core-shell particles being more spherical and having a smaller diameter than the shellac particles from monoaxial electrospraying.

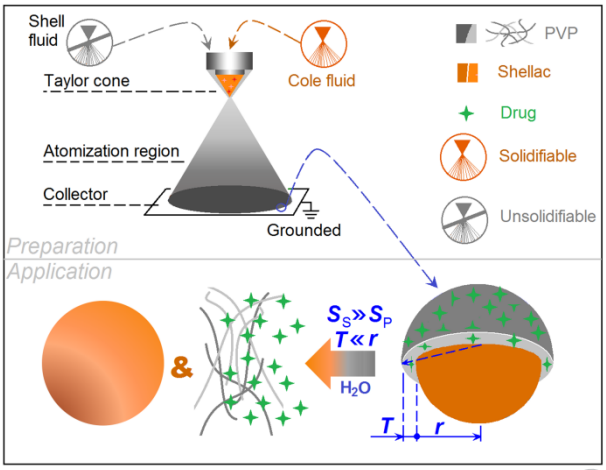

Fig. 8 The mechanism for generating the nanocoating and its fast dissolution properties.

From the sphere volume, $V=4/3\pi r^3$, the volume of the shell section can be estimated based on the particle diameter and shell thickness. The radius of the P2 particles is 355 nm (r=710/2 nm), and the average thickness of the shell T=7 nm. The volume of a single particle is $4/3\pi\times355^3$, and the volume of the coating at the particle's surface is $4/3\pi\times(355^3-348^3)$. The ratio of the overall particle volume to the shell volume is 17.3 times.

The dissolution rate (dQ/dt) of materials can be estimated through the Noyes-Whitney equation [57] :

$$dQ/dt=(A\times D)/h\times(C_s-C_t) \qquad \text{(Equation 3)}$$

Where Q denotes the amount of drug in the dissolving media, t the time, and A, D, h, C_s and C_t denote the effective surface area, the drug diffusion coefficient, the distance of the effective diffusion boundary layer, the saturation solubility of drug, and the drug concentration in the dissolution medium at time t, respectively. Based on this equation, it is clear that the drug dissolution rate is directly proportional to the surface area (A) but inversely proportional to the thickness of the diffusion boundary layer (h). In this study, change in h can be estimated as 7/355. The surface area increased 17.3 times. Thus, the theoretical dQ/dt increase is 17.3×355/7=877-fold.

3.6. Perspectives

Building on recent advances in traditional and modified coaxial electrospinning, here modified coaxial electrospraying is explored as a novel concept for EHDA processes. Several previous publications have demonstrated that, with a solvent as the shell fluid, modified coaxial electrospraying can manipulate the resultant particles' shape and size, and prevent spray head clogging during working processes [20,21,24]. However, they did not result in any novel architectures or structural characteristics. Here, we expand the capability of electrospraying to generate new nanostructures.

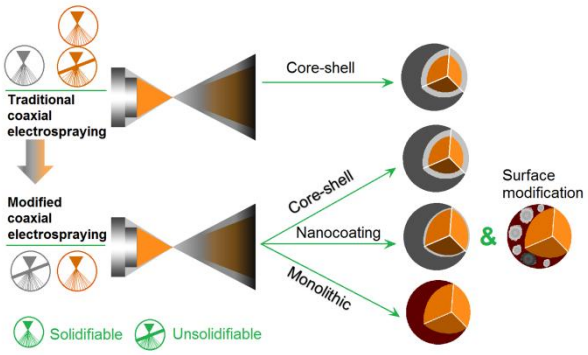

Fig. 9 A diagram depicting the potential applications of coaxial and modified coaxial electrospraying.

A diagram comparing the potential applications of coaxial and modified coaxial electrospraying is exhibited in Fig. 9. In traditional coaxial electrospraying, the shell working fluid must be solidifiable to yield solid particles. The products are particles with solid shells and a variable core. In modified coaxial electrospraying, the core fluid is solidifiable, but the shell fluid cannot be converted into solid particles in a one-fluid electrospraying process. There are numberous un-solidifiable fluids, as compared to a smaller number of solidifiable solutions. Accordingly, the modified process lends itself to more possibilities than the traditional variant. In addition to the solid core-shell particles, the modified process can also exploited to give particles with very thin nanocoatings, as in this work. In future, it is possible that the technology could be developed such that the coating is composed of a single layer of molecules. In addition, other unsolidifiable

liquids such as nanosuspensions and emulsions could also be explored as the shell fluid, resulting in a range of surface modifications. If the shell fluid is a plain solvent, the modified process can generate higher quality monolithic particles, in terms of their diameter and size distribution, and surface smoothness [20,21,24].

4. Conclusions

A new strategy to prepare high-performance nanomaterials is demonstrated in this work. Core/shell nanoscale particles were prepared in which a very thin shell layer was employed to give very rapid dissolution of a poorly water soluble drug. A new modified coaxial electrospraying process was developed to this end. This employed a PVP-helicid solution as the shell, and shellac as the core. Electrospraying resulted in a thin solid nanocoating (estimated thickness 7 nm) on the shellac particles. The drug was amorphously dispersed in the PVP matrix thanks to favorable hydrogen bonding between the molecules, as demonstrated by FTIR results. *In vitro* dissolution experiments showed that all the helicid content can be released into solution within 1 min, a speed two orders of magnitude faster than pure helicid. Modified coaxial electrospraying can hence greatly extend the ability of electrospraying to produce novel nanostructures, exploiting numerous working fluids that cannot be processed using a one-fluid process, and providing new strategies for fabricating novel functional materials.

Acknowledgements:

The authors gratefully acknowledge financial support from the Natural Science Foundation of China (Grant Ref. 51373101).

References

[1] B. P. Isaacoff, K. A. Brown, Progress in top-down control of bottom-up assembly, Nano Lett. 17 (2017) 6508-6510.

[2] J. A. Hubbell, A. Chikoti, Nanomaterials for drug delivery, Science 337 (2012) 303-305.

[3] S. Chakraborty, I. C. Liao, A. Adler, K. W. Leong, Electrohydrodynamics: a facile technique to fabricate drug delivery systems, Adv. Drug Deliver. Rev. 61 (2009) 1043-1054.

[4] Z. Mao, J. L. Li, W. J. Huang, H. Jiang, B. L. Zimba, L. Chen, J. L. Wan, Q. Z. Wu, Preparation of poly(lactic acid)/graphene oxide nanofiber membranes with different structures by electrospinning for drug delivery, RSC Adv. 8 (2018) 16619-16625.

[5] D.H. Kang, H. W. Kang, Advanced electrospinning using circle electrodes for freestanding PVDF nanofiber film fabrication, Appl. Surf. Sci. 455 (2018) 251–257.

[6] M. Eltayeb, E. Stride, M. Edirisinghe, A. Harker, Electrosprayed nanoparticle delivery system for controlled release, Mater. Sci. Eng. C 66 (2016) 138-146.

[7] J. Y. Lee, C. Crake, B. Teo, D. Carugo, M. de Saint Victor, A. Seth, E. Stride, Ultrasound-enhanced siRNA delivery using magnetic nanoparticle-loaded chitosan-deoxycholic acid nanodroplets, Adv. Healthcare Mater. 6 (2017) 1601246.

[8] A. Khalf, S. V. Madihally, Recent advances in multiaxial electrospinning for drug delivery, Eur. J. Pharm. Biopharm. 112 (2017) 1-17.

[9] D.H. Kang, H. W. Kang, Surface energy characteristics of zeolite embedded PVDF nanofiberfilms with electrospinning process, Appl. Surf. Sci. 387 (2016) 82-88.

[10] S. H. Jiang, G. G. Duan, E. Zussman, A. Greiner, S. Agarwal, Highly flexible and tough concentric tri-axial polystyrene fibers, ACS Appl. Mater. Interfaces 6 (2014) 5918-5923.

[11] S. Agarwal, A. Greiner, J. H. Wendorff, Functional materials by electrospinning of polymers, Prog. Polym. Sci. 38 (2013) 963-991.

[12] M. Eltayeb, E. Stride, M. Edirisinghe, Electrosprayed core–shell polymer–lipid nanoparticles for active component delivery, Nanotechnology 24 (2013) 465604.

[13] J. D. Starr, J. S. Andrew, Janus-type bi-phasic functional nanofibers, Chem. Comm. 49 (2013) 4151-4153.

[14] H. Jiang, G. G. Duan, E. Zussman, A. Greiner and S. Agarwal, Highly flexible and tough concentric triaxial polystyrene fibers, ACS Appl. Mater. Interfaces 6 (2014) 5918-5923.

[15] D. Han, S. Sherman, S. Filocamo, A. J. Steckl, Long-term antimicrobial effect of nisin released from electrospun triaxial fiber membranes, Acta Biomater. 53 (2017) 242-249.

[16] C. Yang, D. G. Yu, D. Pan, X. K. Liu, X. Wang, S. W. Annie Bligh, G. R. Williams, Electrospun pH-sensitive core-shell polymer nanocomposites fabricated using a tri-axial processes, Acta. Biomater. 35 (2016) 77-86.

[17] X. Liu, Y. Yang, D. G. Yu, M. J. Zhu, M. Zhao, G. R. Williams, Tunable zero-order drug delivery systems created by modified triaxial electrospinning, Chem. Eng. J. 356 (2019) 886-694.

[18] Y. Yang, W. Li, D. G. Yu , G. Wang, G. R. Williams, Z. Zhang, Tunable drug release from nanofibers coated with blank cellulose acetate layers fabricated using tri-axial electrospinning, Carbohydr. Polym. 203 (2019) 228-237.

[19] S. Labbaf, H. Ghanbar, E. Stride, M. Edirisinghe, Preparation of multilayered polymeric structures using a novel four-needle coaxial electrohydrodynamic device, Macromol. Rapid Comm. 35 (2014) 618-623.

[20] Z. P. Liu, L. L. Zhang, Y. Y. Yang, D. Wu, G. Jiang, D. G. Yu, Preparing composite nanoparticles for immediate drug release by modifying electrohydrodynamic interfaces during electrospraying, Powder Technol. 327 (2018) 179-187.

[21] X. Y. Li, Z. B. Zheng, D. G. Yu, X. K. Liu, Y. L. Qu, H. L. Li, Electrosprayed sperical ethylcellulose nanoparticles for an improved sustained-release profile of anticancer drug, Cellulose 24 (2017) 5551-5564.

[22] Sayed, C. Karavasili, K. Ruparelia, R. Haj-Ahmad, G. Charalambopoulou, T. Steriotis, D. Giasafaki, P. Cox, N. Singh, L.-P. N. Giassafaki, A. Mpenekou, C. K. Markopoulou, I. S. Vizirianakis, M.W. Chang, D. G. Fatouros, Z. Ahmad, Electrosprayed mesoporous particles for improved aqueous solubility of a poorly water soluble anticancer agent: in vitro and ex vivo evaluation, J. Control. Release 278 (2018) 142-155.

[23] Zhang, Z. C. Yao, Q. Ding, J. J. Choi, Z. Ahmad, M. W. Chang, J. S. Li, Tri-needle coaxial electrospray engineering of magnetic polymer yolk-shell particles possessing dual-imaging modality, multiagent compartments, and trigger release potential, ACS appl. Mater. Interfaces 9 (2017) 21485-21495.

[24] Z. P. Liu, Y. Y. Zhang, D. G. Yu, D. Wu, H. L. Li, Fabrication of sustained-release zein nanoparticles via modified coaxial electrospraying, Chem. Eng. J. 334 (2018) 807-816.

[25] Q. Wang, D. G. Yu, L. L. Zhang, X. K. Liu, M, Zhao, Electrospun hypromellose-based hydrophilic composites for rapid dissolution of poorly water-soluble drug, Carbohyd. Polym. 174 (2017) 617-625.

[26] Y. Y. Yang, M. Zhang, K. Wang, D. G. Yu, pH-sensitive polymer nanocoating on hydrophilic composites fabricated using modified coaxial electrospraying, Mater. Lett. 227 (2018) 93-96.

[27] Y. Liao, C. H. Loh, M. Tian, R. Wang, A. G. Fane, Progress in electrospun polymeric nanofibrous membranes for water treatment: Fabrication, modification and applications, Prog. Polym. Sci. 77 (2018) 69-94.

[28] I. G. Loscertales, A. Barrero, I. Guerrero, R. Cortijo, M. Marquez, A. M. Ganan-Calvo, Micro/nano encapsulation via electrified coaxial liquid jets, Science 295 (2002) 1695-1698.

[29] Y. Gao, D. Zhao, M. W. Chang, Z. Ahmad, J. S. Li, Optimising the shell thickness-to-radius ratio for The Fabrication of oil-encapsulated polymeric microspheres, Chem. Eng. J. 284 (2016) 963-971.

[30] J. H. Yang, G. Z. Yang, D. G. Yu, X. Wang, B. Zhao, L. L. Zhang, P. Du, X. K. Zhang, Carbon foams from polyacrylonitrile-borneol films prepared using coaxial electrohydrodynamic atomization, Carbon 53 (2013) 231-236.

[31] R. G. Chaudhuri, S. Paria, Core/shell nanoparticles: classes, properties, synthesis mechanisms, characterization, and applications, Chem. Rev. 112 (2012) 2373-2433.

[32] N. Kamaly, B. Yameen, J. Wu, O. C. Farokhzad, Degradable controlled-release polymers and polymeric nanoparticles: mechanisms of controlling drug release, Chem. Rev. 116 (2016) 2602-2663.

[33] E. Pavitra, G. S. R. Raju, G. P. Nagaraju, G. Nagaraju, Y. K. Han, Y. S. Huh, J. S. Yu, TPAOH assisted size-tunable Gd_2O_3@ mSi core–shell nanostructures for multifunctional biomedical applications, Chem. Commun. 54 (2018) 747-750.

[34] Rogina, Electrospinning process: Versatile preparation method for biodegradable and natural polymers and biocomposite systems applied in tissue engineering and drug delivery, Appl. Surf. Sci. 296 (2014) 221-230.

[35] G. Chen, Y. Wang, R. Xie, S. Gong, A review on core–shell structured unimolecular nanoparticles for biomedical applications, Adv. Drug Deliv. Rev. (2018) https://doi.org/10.1016/j.addr.2018.07.008.

[36] L. Jiang, L. Wang, N. Wang, S. Gong, L. Wang, Q. Li, C. Shen, L.S. Turng, Fabrication of polycaprolactone electrospun fibers with different hierarchical structures mimicking collagen fibrils for tissue engineering scaffolds, Appl. Surf. Sci. 427 (2018) 311-325.

[37] D. G. Yu, J. J. Li, G. R. Williams, M. Zhao,Electrospun amorphous solid dispersions of poorly water-soluble drugs: A review. J. Control. Release, 2018, https://doi.org/10.1016/j.jconrel.2018.08.016.

[38] W. Liang, J. Hou, X. Fang, F. Bai, T. Zhu, F. Gao, C.Wei, X.M. Mo, M. Lang, Synthesis of cellulose diacetate based copolymer electrospun nanofibers for tissues scaffold, Appl. Surf. Sci. 443 (2018) 374-381.

[39] A. Balogh, A. Domokos, B. Farkas, A. Farkas, Z. Rapi, D. Kiss, Z. Nyiri, Z. Eke, G. Szarka, R. Örkényia, B. Mátravölgyia, F. Faigla, G. Marosia, Z. K. Nagya, Continuous end-to-end production of solid drug dosage forms: Coupling flow synthesis and formulation by electrospinning, Chem. Eng. J. 350 (2018) 290-299.

[40] C. Le-Ngoc Vo, C. Park, B. J. Lee, Current trends and future perspectives of solid dispersions containing poorly water-soluble drugs, Eur. J. Pharm. Biopharm. 85 (2013) 799-813.

[41] Z. K. Nagy, A. Balogh, B. Demuth, H. Pataki, T. Vigh, B. Szabó, K. Molnár, B. T. Schmidta, P. Horák, G. Marosi, G. Verreck, I. V. Assche, M. E. Brewster, High speed electrospinning for scaled-up production of amorphous solid dispersion of itraconazole, Int. J. Pharm. 480 (2015) 137-142.

[42] K. Wang, X. K. Liu, X. H. Chen, D. G. Yu, Y. Y. Yang, P. Liu, Electrospun hydrophilic Janus nanocomposites for the rapid onset of therapeutic action of helicid, ACS Appl. Mater. Interfaces 10 (2018) 2859−2867.

[43] M. N. Siddiqui, G. Garg, P. K. Sharma, A novel approach in oral fast dissolving drug delivery system and their patents, Adv. Biol. Res. 5 (2011) 291-303.

[44] J. J. Li, Y. Y. Yang, D. G. Yu, Q. Du and X. L. Yang, Fast dissolving drug delivery membrane based on the ultra-thin shell of electrospun core-shell nanofibers, Eur. J. Pharm. Sci. 122 (2018) 195-204.

[45] B. Démuth, A. Farkas, B. Szabó, A. Balogh, B. Nagy, E. Vágó, T. Vigh, A. P. Tinke, Z. Kazsu, Á. Demeter, J. Bertels, J. Mensch, A.Van Dijck, G.Verreck, I. V. Assche, G. Marosi, Z. K. Nagy, Development and tableting of directly compressible powder from electrospun nanofibrous amorphous solid dispersion, Adv. Powder Technol. 28 (2017) 1554-1563.

[46] A. Hermans, A. M. Abend, F. Kesisoglou, T. Flanagan, M. J. Cohen, D. A. Diaz, Y. Mao, L. Zhang, G. K. Webster, Y. Lin, D. A. Hahn, C. A. Coutant, H. Grady, Approaches for establishing clinically relevant dissolution specifications for immediate release solid oral dosage forms, AAPS J. 19 (2007) 1537-1549.

[47] S. Mei, P. P. Han, H. Wu, J. F. Shi, L. Tang, Z. Y. Jiang, One-pot fabrication of chitin-shellac composite microspheres for efficient enzyme immobilization, J. Biotechnol. 266 (2018) 1-8.

[48] B. Saberi, S. Chockchaisawasdee, J. B. Golding, C. J. Scarlett, C. E. Stathopoulos, Development of biocomposite films incorporated with different amounts of shellac, emulsifier, and surfactant, Food Hydrocolloid. 72 (2017) 174-184.

[49] N. Pearnchob, J. Siepmann, R. Bodmeier, Pharmaceutical applications of shellac: moisture-protective and taste-masking coatings and extended-release matrix tablets, Drug Dev. Ind. Phar. 29 (2003) 925-938.

[50] K. Wang, H. F. Wen, D. G. Yu, Y. Y. Yang, D. F. Zhang, Electrosprayed hydrophilic nanocomposites coated with shellac for colon-specific delayed drug delivery, Mater. Design 143 (2018) 248-255.

[51] Y. Y. Yang, Z. P. Liu, D. G. Yu, K. Wang, P. Liu, X. H. Chen, Colon-specific pulsatile drug release provided by electrospun shellac nanocoating on hydrophilic amorphous composites, Int. J. Nanomed. 13 (2018) 2395-2404.

[52] M. Q. Zhang, T. X. Wang, R. Li, Z. L. Huang, W. J. Han, X. C. Dai, Y. Q. Wang, Helicid alleviates pain and sleep disturbances in a neuropathic pain-like model in mice, J. Sleep Res., 26 (2017) 386-393.

[53] Y. W. Jia, J. Shen, J. G. Sun, W. Wang, H. Xie, Bioavailability and pharmacokinetics profile of helicid in beagle dogs using gradient elution high performance liquid chromatography electrospray ionization mass spectrometry, J. Chromatogr. B 988 (2015) 8-12.

[54] L. Paniwnyk, E. Beaufoy, J. P. Lorimer, T. J. Mason, The extraction of rutin from flower buds of Sophora japonica, Ultrason. Sonochem. 8 (2001) 299-301.

[55] W. Nie, The new application of shellac in drug delivery system, Master dissertation Jan-9, 2012, Shanghai, China.

[56] V. Salata, Tools of nanotechnology: Electrospray, Curr. Nanosci. 1 (2005) 25-33.

[57] D. E. Wurster, P. W. Taylor, Dissolution rates, J. Pharm. Sci. 54 (1965) 169-175.

Graphical abstract

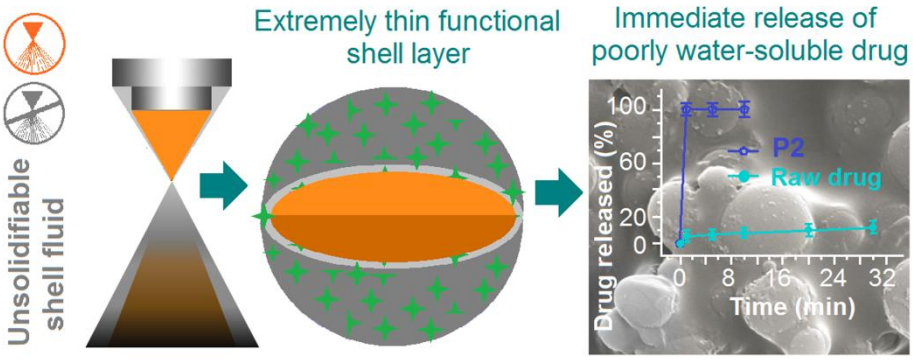

Highlights

- A strategy was shown for enhancing the dissolution of poorly water-soluble drug
- A modified coaxial electrospraying was developed
- Unsolidifiable solution was explored as shell working fluid
- Extremely thin composite functional shell was built on a blank core
- Immediate release of helicid due to nanoeffects provided by a thin surface layer